Chapter 9

Vortex cavitation

Objective: *Description of the structure of a cavitating vortex and its appearance on ship propellers*

Vortices are important for ship propellers because the pressure in the core is low and thus cavitation may occur. Vortex cavitation is not erosive when it is not excessive, but it is a source of noise. And noise is used to detect ships and is thus important for navy ships. Radiated noise was and is used to find the location of ships. Since low frequency noise reaches longer distances these frequencies were detected with towed arrays. This detection method has been replaced by detection by satellites. However, for close range detection noise is still very important, because the main target of torpedoes is a noise source. Tip vortex inception often determines the speed at which the propeller starts to radiate cavitation noise, which remains important for navy ships.

There is also increased interest in cavitation inception of commercial ships because of the suspected interference of the radiated noise with marine life. Although very little is known about the relation between noise and biological damage, there is a tendency to reduce noise radiation. Especially cruise ships want are keen on having a green label, so they want to operate without cavitation.

As a whole, tip vortex cavitation is therefore important for navy ships and for research vessels which have to operate without self-noise. Developed tip vortex cavitation is not very critical in general, except when it is excessive. The dynamics of cavitating tip vortices are still poorly understood, but it is likely that these dynamics play a rle in broadband noise radiated in some cases and in cavitation induced pressure fluctuations. These induced pressures may be influenced by the interaction between sheet cavitation and the cavitating tip vortex.

Inception of vortices is an important issue for model testing, because cavitation inception of a vortex is strongly dependent on the Reynolds number. As a result, tip vortex cavitation occurs much later at model scale than at full scale, and this can lead to large errors in the prediction of cavitation.

To understand vortex cavitation it is necessary to understand the structure and representation of the non-cavitating vortex first. A vortical flow structure can be described in terms of flow velocities by the shape of the streamlines. A vortical structure is a circulating flow in a certain plane in a fluid, which means that the flow lines are closed. The closed streamlines have to contain only fluid, because when there is a body in the closed streamlines there is not a vortex but we regard it as circulation around the body.

9.1 Vortex, vorticity and vortex induced velocities

It is, however, more convenient to describe the flow in terms of *vorticity* instead of in terms of velocities. Then a vortex is defined as *a concentration of vorticity.*

9.1.1 Vorticity

Vorticity is defined as rotation of fluid elements. Vorticity is generated by friction forces in the fluid, as follows from the consideration of forces on an infinitesimal small fluid element. In an inviscid fluid there are only pressure forces acting on a fluid element (Fig.9.1). The fluid element will deform due to these forces, but will not rotate. Without rotation the equations of motion are described by the Laplace equation. (Note: When there is rotation at time t in an inviscid fluid, the rotation will not change due to the pressure forces, but it can be changed by fluid accelerations in the z-direction. The governing equation of motion is the Euler equation). Rotation is only generated by frictional forces, as shown in Fig.9.2. The fluid element at time t+dt is not only deformed, but also rotated, which is measured by the average angle of the bisectrices of the element.

Vorticity is defined as the curl of the equation of motions, and in two dimensions it is written as

$$\omega = \frac{\partial u}{\partial y} - \frac{\partial v}{\partial x} \tag{9.1}$$

which is twice the angular velocity of the fluid element in Fig.9.2. Vorticity is defined in a plane and it is thus a vector,which means that it has not only a strength but also a direction.

When a vortex is defined in terms of vorticity, a vortex is a *concentration of vorticity in one direction* in a body of fluid. In Fig. 9.3 a cross section of the fluid perpendicular to the direction of the vorticity is given. The strength of the vorticity has been indicated by the intensity of the color. In the center there is a strong vorticity, around the center the vorticity is lower and in the region between streamlines C and D there is no vorticity, as in the region outside D.

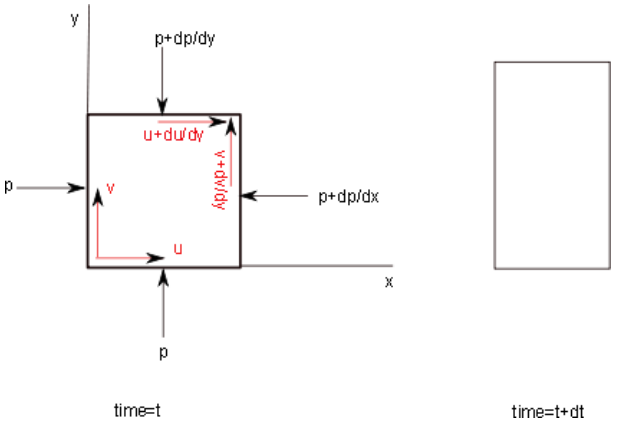

Figure 9.1: Deformation of a fluid element due to pressure forces

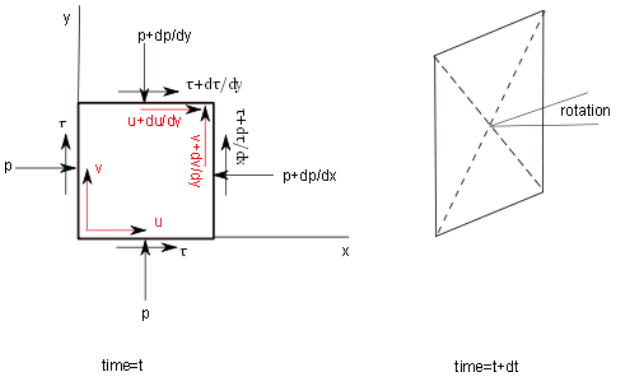

Figure 9.2: Defprmation and rotation of a fluid element due to pressure and friction forces

A measure of the strength of a vortical structure is the *circulation* Γ. This is the integral of the velocity over a closed streamline (Stokes'

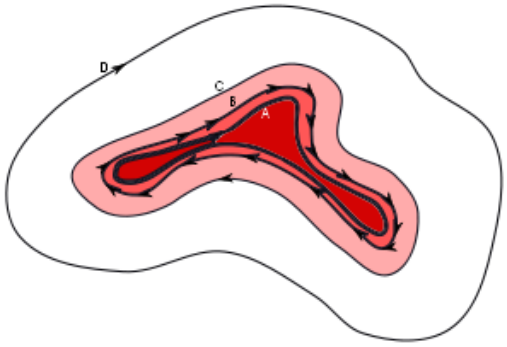

Figure 9.3: The structure of a vortex

law).

$$\Gamma = \int V ds \tag{9.2}$$

where s is the closed streamline. The circulation also is the integral of the vorticity over the area of the closed streamline, so

$$\Gamma = \int \omega da \tag{9.3}$$

in which a is the area inside the streamline. As long as there is vorticity between various streamlines the circulation will change with the streamline.

When the vorticity between two contours is zero (as between streamlines C and D in Fig. 9.3) the circulation of both contours is the same. The circulation around streamlines A, B and C will be increasing. The strength of a vortex Γ is now defined by its maximum circulation. The location of a vortex is generally taken somewhere in the center of the region with vorticity. Since vorticity has the tendency to roll-up into a cylindrical shape this is often not very difficult.

Note that the description above assumes that there is one vortex under consideration. The situation is much more complex in e.g. a boundary layer. There the vorticity occurs in many directions and scales and it can be difficult to distinguish coherent vortical structures (e.g.[26]). This can also occur in the collapse region of a cavity, where multiple vortices are interacting with each other. In our discussions we will focus, however, on single vortices, eventually interacting with distinct other vortices.

9.1.2 Vortex induced velocities

A vortex can now be divided into two regions. The first region is the vortex core, which is the region with vorticity. This vortex core is often indicated as the vortex itself. The second region is the region outside the vortex core, where there is no vorticity. These velocities are therefore called *vortex induced velocities*, although it would be better to talk about vortex core induced velocities. The term induced is used because the relation between the vortex core and the velocities outside the core is similar as in a magnetic field. The mechanism which establishes this induction in a flow field is viscosity. It is important to note that a vortex consists both of a vortex core and of induced velocities outside the core. Both are components of one vortex and are directly linked to each other. There is also no strict limit to the extension of a vortex. Its extension is infinite, although at larger distances from the core the induced velocities become negligibly small.//

In an incompressible flow without viscosity the circulation in a body of fluid remains constant (Thomson's law). The body of fluid can, however be transformed and translated. This means that the vorticity can be changed over time. An example is the *stretching* of a vortex when the vortex exists in an accelerating flow. The strength of the vortex remains the same, but the radius decreases, resulting in an increase of the local vorticity

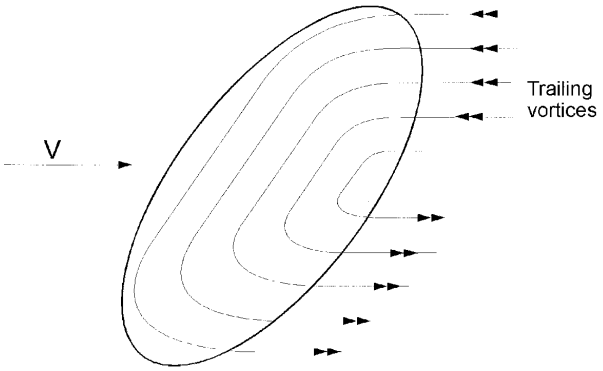

Figure 9.4: Vorticity downstream of a lifting wing

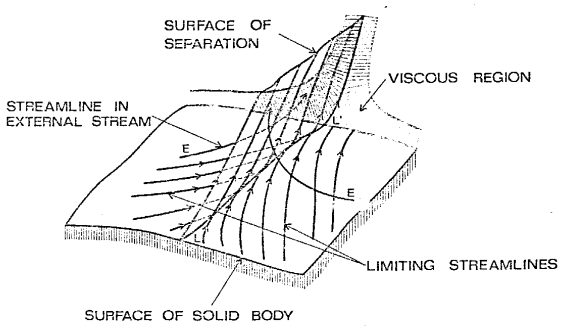

Figure 9.5: Vorticity generated by longitudinal separation in a boundary layer

in the core. The location of the vortex is defined by the translation of the fluid element, which means that a vortex moves with the (local)flow.

9.1.3 The source of vorticity

As has been mentioned vorticity is generated in a boundary layer, where large velocity gradients occur. So viscosity is a necessity for the generation of vorticity. A vortex is defined as a concentration of vorticity in *free* flow. So there has to be separation to generate a vortex. Examples are the wake of a wing with a certain spanwise loading distribution (Fig. 9.4). Near the trailing edge of the wing there is separation (the Kutta condition in potential flow) and a plane of vorticity occurs in the separated flow at the trailing edge. Separation can also occur in flow direction, as is often the case with bilge vortices (Fig. 9.5). Here also vorticity is released in the free flow. In both examples the vorticity is in a plane, but will soon roll-up, as will be discussed later.

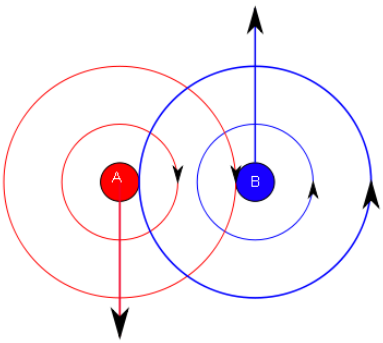

Figure 9.6: Vortex roll-up of two separate vortices

9.1.4 Vortices behind a wing

Co-rotating vortices have the tendency to roll up into a more or less cylindrical shape. This can be explained by considering two schematic vortices A and B as in Fig. 9.6.

Vortex A will follow the streamline of vortex B. Vortex B will follow the streamline of vortex A. As a result they will rotate around each other and eventually form a single vortex.

A well known example is the roll-up of the vortex plane behind a wing, as given in Fig. 9.4. This plane develops as in Fig 9.7. The ends roll up and develop into a tip vortex, in which the core has a spiral structure. The result is a tip vortex with a vorticity distribu-

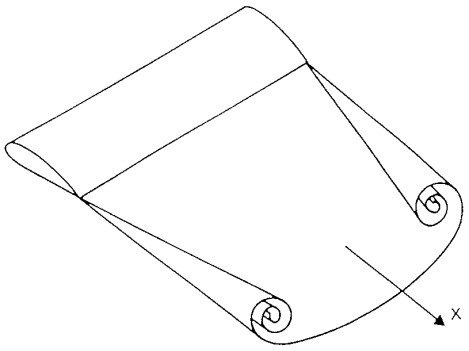

Figure 9.7: Vortex roll-up behind a wing

tion and strength depending on the distance from the wing.

To get an idea about the amount of roll-up behind a wing we will consider an wing with an elliptical contour, because its loading can be treated analytically. The spanwise circulation distribution is

$$\Gamma(x) = \Gamma_0(1 - x^2)^{0.5} \tag{9.4}$$

where x is the spanwise position, made non-dimensional with the semi-span and Γ_0 is the maximum circulation at the center of the wing.

At the trailing edge of the wing a free vortex sheet is formed with a strength of $\omega(x) = \frac{\delta\Gamma(x)}{\delta(x)}$The strength of the trailing vortex sheet over the span is then

$$\omega(x) = -\Gamma_0 x(1 - x^2)^{-0.5} \tag{9.5}$$

A problem in calculations is that the strength at the tip is infinite, but the integral over a finite distance from the tip to the tip is finite. So when the trailing vortex is discretized, the strength of the last element at the tip remains finite. An example of the development of a trailing vortex behind an elliptical wing is given by Moore [48].

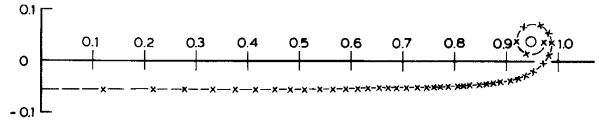

Figure 9.8: Spanwise distribution of trailing vortices behind a wing (Moore 1974)

He divided the vortex sheet in 60 discrete vortices of equal strength γ. The distance of these vortices can then be found from $Rx = \frac{\gamma}{\omega(x)}$. Initially these vortices are widely spaced near the center, and become more densely spaced towards the tip. Figure 9.8 shows the position of these vortices in a plane at 5% of the half wing span downstream of the initial position. An approximation of the tip vortex strength due to roll-up was already given by Kaden [29] as

$$\Gamma(tip) = gy^{1/3}\Gamma_0 \tag{9.6}$$

for y smaller than 0.1. Here y is the distance behind the wing, made non-dimensional with the semi-span. The value of g is close to 1. At y=0.1 this means that 46% of the total trailing vorticity is present in the tip vortex. Moore calculated complete roll-up at about $y = 10$, but at $y = 1$ already 80% of the circulation was rolled-up. In case of a propeller the semi-span of the wing is about 0.7R (R is the propeller radius). So with a similar loading as an elliptic wing 80 percent of the trailing vorticity is rolled-up within a distance of 0.7R behind the tip. In terms of a rotating propeller blade this is within a blade rotation of 40 degrees.

9.2 Modeling the velocities in a cylindrical vortex

In a vortex the main velocity component is perpendicular to the vortex center. Therefore

two-dimensional vortex models are used to describe the velocity field. Some classical simple models will be discussed now. The aim is to show the main properties of a vortex. The accuracy of these models is very limited.

Assume a vortex with all vorticity concentrated in an infinitely small circle in a plane perpendicular to the vortex. The strength of the vortex is Γ. Now let the radius of the vortical region go to zero while maintaining the strength of the vortex. This leads to a singular behavior in the center of the vortex, because the velocities become infinite. Also the notion of vorticity and its distribution loses its meaning since al vorticity is contained in one point. Such a velocity field is called a Rankine vortex (although sometimes a vortex with a solid core of finite diameter is called the same). The flow field around such a vortex is now determined by Γ alone. Since the circulation at every radius is the same, the tangential velocity around the vortex is

$$V_r = \frac{\Gamma}{2\pi r} \tag{9.7}$$

The flow away from the center has a moderate velocity gradient, so the effect of viscosity can be neglected, at least over a short time span. Since there is no vorticity, the outer flow of a vortex is a *potential flow field*. This means that the flow fields of several vortices can be added and the outer flow of Fig. 9.3 can thus be described by a distribution of Rankine vortices.

It is clear that close to the vortex this model is not physically realistic, as is indicated by the fact that the flow velocity in the core of a Rankine vortex is infinite.

Consider now a situation in which the vorticity is distributed in the center of the vortex, as in Fig.9.9. Symmetry requires that in the center of the vortex the tangential velocity should be zero.

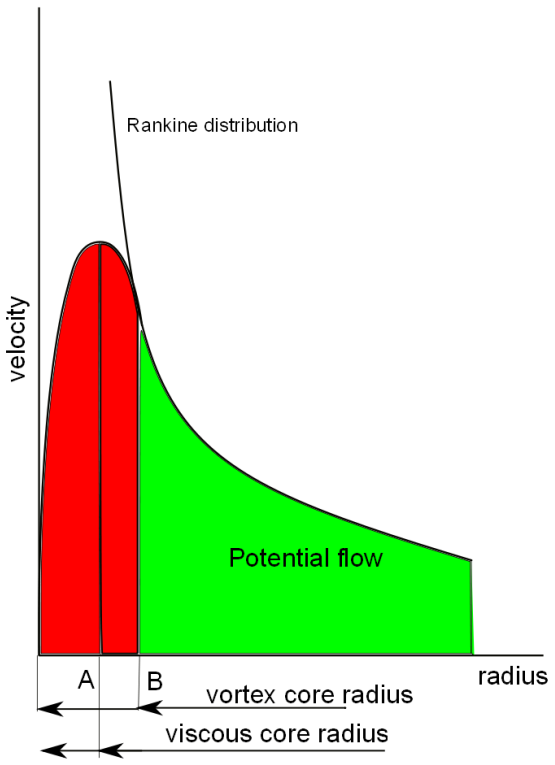

Figure 9.9: The velocity distribution in a cylindrical vortex

In the outer region there is no vorticity and the Rankine velocity distribution (eq.9.7) exists. The strength of the vortex is the integral of the vorticity, so the strength of the vortex is the circulation at radius B. Inside radius B the velocity gradient becomes so high that viscosity becomes more important. It will slow down the tangential velocity. This results in a certain distribution of vorticity in the center of the vortex, which corresponds with a velocity distribution inside radius B. When the vortex core is defined as the region with vorticity, the vortex core radius is radius B. From radius B inward the velocity distribution will deviate from the Rankine distribution because the circulation decreases at smaller radii (because there is vorticity in the radius between A and B the integral

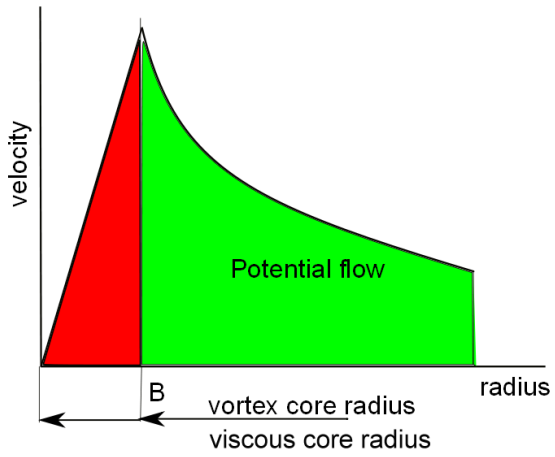

Figure 9.10: The velocity distribution in a vortex with a solid core rotation

decreases with decreasing radius). This leads to zero tangential velocity at the vortex center.

At a radius of about $1.12\sqrt{4\nu t}$ the tangential velocity will have a maximum (radius A). This radius is often defined as the viscous core radius. Strictly speaking this is confusing, because the vorticity distribution between radius A and B is also generated by viscosity. But radius A is used as the core radius because it can be determined from the measured velocity field.

A simplified case is when outside radius A there is no vorticity. Such a case is given in Fig. 9.10. With a linear distribution of vorticity inside radius B the core rotates like a solid body. It is clear that this situation is only a crude approximation of the real. The velocity distribution as in Fig. 9.10 is sometimes also called a Rankine vortex.

A more realistic velocity distribution is the velocity distribution which is found from the Navier Stokes equation for laminar flow, starting from a Rankine vortex ([43]). In the center of the vortex the velocity gradients are huge and viscosity will cause an outward dissipation of vorticity. After some time the tangential velocity distribution which is obtained has the shape of Fig. 9.9 and is formulated as:

$$v(r) = \frac{\Gamma}{2\pi r}[1 - e^{-\frac{r^2}{4\nu t}}] \tag{9.8}$$

This illustrates the asymptotic nature of the vorticity distribution in radial direction.

In the foregoing the outer flow of a vortex has been considered as irrotational (no vorticity). The question is if that corresponds to physical flows because there is a velocity gradient in radial direction in the outer flow, which will generate vorticity. Only when the viscosity is negligible, irrotational flow is possible. Irrotational flow means that the flow particles do not rotate, and a fluid particle will thus move around the vortex center without changing its position. This is illustrated by the fluid particles A and B in Fig. 9.11. When these particles are in position A1 and B1 their orientation is the same as in position A2 and B2. This seems counterintuitive, because a body is expected to rotate around the vortex core. This, however, is still the case, because the rotation refers to infinitely small fluid particles. A body with extension AB will still rotate due to the velocity gradient between the two radii of particles A and B. So even though the irrotational outer flow is an approximation (the real fluid is viscous and a very slight rotation will occur), the approximation of the translation velocities is still accurate.

9.3 The pressure distribution in a vortex

The pressure distribution in the center of a vortex is lower than in the surrounding fluid because of the centrifugal effects of the rotating fluid. In a cylindrical vortex this can easily be derived from the force equilibrium on a fluid

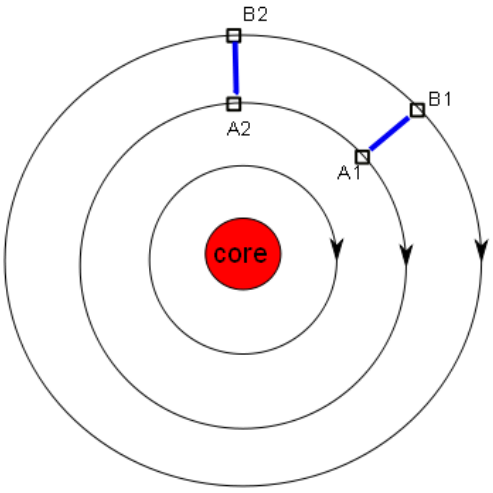

Figure 9.11: The motion of fluid particles and of bodies in an irrotational flow around a vortex

particle in the rotating flow. A rotating particle with follows a cylindrical path around the vortex core is subject to a centrifugal force on a fluid element $\rho r dr d\phi$, which has to be compensated by the pressure force in radial direction

$$\frac{\partial p}{\partial r} = \rho \frac{v^2(r)}{r} \tag{9.9}$$

In the case of a Rankine vortex as in eq. 9.7, integration over r from a radius a $r = a$ to $r = \infty$ results in

$$p_\infty - p_(a) = \frac{\rho \Gamma^2}{4\pi^2 a^2} \tag{9.10}$$

In the center of the vortex $a = 0$ and the pressure difference goes to infinity, so the minimum pressure of a simple rankine vortex is meaningless. With a solid core rotation, as in Fig. 9.10 the velocity distribution inside the core is

$$v(r) = \frac{\Gamma r}{2\pi a_v^2} \tag{9.11}$$

the pressure drop in the core is

$$p_{min} - p_a = \frac{\rho \Gamma^2}{4\pi} \tag{9.12}$$

and thus independent of the viscous core radius.
The minimum pressure in the vortex center is

$$p_\infty - p_{min} = \frac{\rho \Gamma^2}{4\pi^2 {a_v}^2} \tag{9.13}$$

in which a_v is the core radius, which is uniquely defined in this case.

In case of a velocity distribution as in Fig. 9.9 the radial velocity distribution is given by equation 9.8. In a similar way the minimum pressure in the vortex core can be calculated analytically to be

$$p_\infty - p_{min} = \frac{\rho \Gamma^2}{4\pi^2} \frac{ln(2)}{4\nu t} \tag{9.14}$$

When the maximum velocities are kept the same ($a_v = 1.12\sqrt{4\nu t}$) the minimum pressure of eq. 9.14 differs from eq. 9.13 only by a factor $ln(2) * 1.12^2 = 0.87$. Because of the presence of the time in eq. 9.14, it also gives a measure of the increase of the minimum pressure with time.

9.4 The structure of a cavitating vortex

The reason for the focus on the minimum pressure in the vortex core is cavitation inception. Let us assume that when the pressure is lower than the vapor pressure water changes into vapor. The volume of vapor is so much larger than the volume of water that the amount of water which evaporates can be neglected. The situation of the cavitating vortex is then as in Fig. 9.12. The vortical fluid is moved outwards

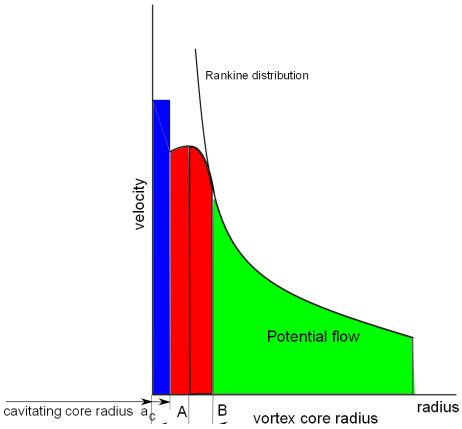

Figure 9.12: The velocity distribution in a cavitating vortex

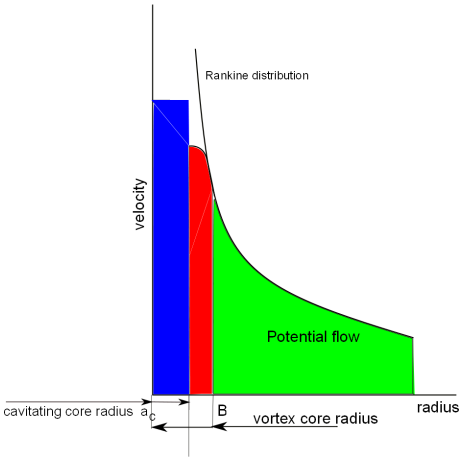

Figure 9.13: The velocity distribution in a cavitating vortex with larger cavitating core

and a vapor region occurs in the vortex center with a radius a_c.

When the cavitating radius increases the radius of the vortical region increases also. Because the total amount of vorticity is constant the thickness of the vortical region decreases rapidly, as sketched in Fig. 9.13.

Ultimately the vortical region will become small and the cavitating vortex has the same shape as the Rankine vortex, but with a vaporous core. Using eq. 9.9 a relation between the cavitating radius, the vortex strength and the outside pressure is found for that case:

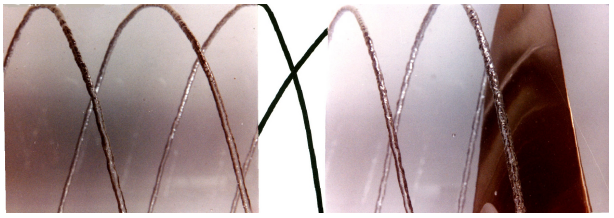

Figure 9.14: The cavitating core of a tip vortex behind a propeller

$$p_\infty - p_v = \frac{0.5\rho\Gamma^2}{4\pi^2 a_c^2} \tag{9.15}$$

Note that a simple replacement of the non-cavitating vortex core with a vaporous core, as in eq. 9.15, does not conserve energy. It assumes that the energy of the non-cavitating vortex core simply disappears. To conserve energy the circulation of the vortex around the cavitating core has to increase.

Equation 9.15 shows that at a certain outside pressure P_∞ the cavitating radius is proportional to the vortex strength. However, observations of a cavitating vortex core behind a propeller blade show that the cavitating vortex core changes very little with distance to the tip (Fig. 9.14 with the flow from right to left) despite a strong increase of the vortex strength due to the roll-up of the trailing vorticity behind the blade.

This shows two important things. First that a significant amount of vorticity has top be present outside the cavitating core, so that the vortex strength can increase with distance to the tip, but the cavitating core radius remains constant or even reduces. The second observation is that there is a very small decrease of the cavitating core over the distance to the tip. This shows that viscous dissipation is very small in the case of a cavitating vortex and inviscid theory can be used.

9.4.1 The relation between the cavitating core radius and the pressure

For a better understanding of the cavitating vortex we take a simple inviscid approach which dates back to Betz in 1931 (from [55]).The bound circulation at a certain position of the wing rolls up into a vortex with a certain radius, as shown in Fig 9.8. Close to the wing tip an arbitrary circulation distribution can be approximated by $\Gamma_b(x) = c_1 x^{1/m}$ where Γ_b is the bound circulation and c_1 represents the wing loading, x is the distance to the tip. For m=2 this is the elliptic loading distribution. Betz assumed that the trailing vortex sheet from a location x to the tip rolls up into a vortex with radius λx and he took λ as a constant. The radial distribution of the circulation can be written as $\Gamma(r) = c_1(\lambda x)^{1/m} = c_1(r)^{1/m}$ for $r < a_v$. This gives a distribution of the red vortical region in Fig. 9.9. Note that in the inviscid case the circulation at the vortex center can be finite. The location and strength of the trailing vortex at some distance from the wing tip can be found from conservation laws such as conservation of vorticity and of moments of vorticity ([55]).

When cavitation inception occurs and the vorticity is maintained the circulation is moved outwards by the vaporous core, and the circulation distribution in the vortical region outside the cavitating core with radius a_c becomes $\Gamma(r) = c_1(r - ac)^{1/m}$ for a_c, r, a_v.. As an example we will consider an elliptical tip loading with $m = 2$. This results in the velocity distribution around the vortex core as:

$$v(r) = \Gamma/2\pi * r \quad r > a_v \tag{9.16}$$

$$v(r) = \frac{\Gamma\sqrt{r - a_c}}{\sqrt{a_v - a_c}2\pi r} \quad a_c < r < a_v \tag{9.17}$$

$$\tag{9.18}$$

where Γ is the maximum circulation in the vortex at radius a_v. Inside a_c there is vapor at the vapor pressure p_v. This is the situation as in Figs. 9.12 and 9.13.

Using eq. 9.9 this gives after some algebra the relation

$$p_\infty - p_v = \frac{\rho\Gamma^2}{8\pi^2 a_v a_c} \tag{9.19}$$

The important aspect of this is that eq. 9.19 gives a rather simple relation between the pressure p_∞ and the cavitating core radius a_c. There is no viscous core in this model, so a_c cannot go to zero. With increasing pressure p_∞ the cavitating core radius goes to zero asypmtotically. Therefore this relation cannot give an inception pressure. But a relation like this can be used to define cavitation inception as the occurrence of a finite minimum cavitating radius, as will be discussed later.

9.5 Inception of tip vortex cavitation

Inception of a vortex is a complicated affair, because it involves a vortex with a low pressure region in the core, but also nuclei to expand in that vortex core. The pressure gradient of a vortex causes nuclei to move towards the vortex center. When such a nucleus reaches a critical pressure it will rapidly expand, but it will also take an elongated shape. But the cavity also moves with the flow and is thus moved away quickly. As a result cavitation inception of a tip vortex begins with flashes of cavitation and is very difficult to discern. The closer we look, the earlier cavitation inception is called. Since one reason to determine cavitation inception of a tip vortex is the radiated noise, it seems reasonable to detect inception acoustically. That is a good method, as long as there are no other cavities or noise sources around. In that case acoustic cavitation inception is found when occasional bursts of noise from the expanding and collapsing nuclei are found. With decreasing pressure the frequency

Figure 9.15: Video:Inception of a tip vortex at high tip loading with stroboscopic illumination

Figure 9.16: Video:Inception of a tip vortex at low tip loading with stroboscopic illumination

of these bursts increases and again a rather arbitrary criterion has to be formulated: the number of bursts per second [23]. Acoustic cavitation inception occurs generally slightly earlier than visual inception. If it occurs later, gaseous cavitation may occur without a violent collapse and thus without noise.

Cavitation inception of a vortex depends strongly on the nuclei content. At model scale it is generally determined with a maximum of nuclei in the cavitation tunnel, but even then inception occurs incidentally, as shown in video 9.15 for a highly loaded tip. In this video the pressure decreases gradually until a cavitating vortex is formed. In such a case the vortex is strong and cavitation develops in a well defined core.

In case of a low tip loading the tip vortex is weak and it requires a much lower pressure to reach inception. The result is a less coherent and more flashy cavitation in the tip vortex, as shown in Fig. 9.16 in which video the pressure again decreases gradually.

To avoid the dominant influence of nuclei, cavitation inception can also be determined when the cavitation disappears. This is called desinent cavitation. In that case a stable tip vortex is first created, as shown in Fig. 9.17.

But when the pressure increases the cavitating core breaks again into small parts, which disappear in different positions and times. In case of steady tip vortex cavitation desinent cavitation has the risk of being gaseous, because the cavitating tip vortex continuously collects nuclei from the fluid together with diffusion from the fluid which is locally supersaturated.

When the inception pressure differs from the pressure at desinence this is called *hysteresis*. Desinent cavitation is shown in Fig. 9.18 (flow from right to left).

Although desinent vortex cavitation is often more reproducible than incipient cavitation, the determination of the precise inception pressure remains difficult and has a considerable error margin.

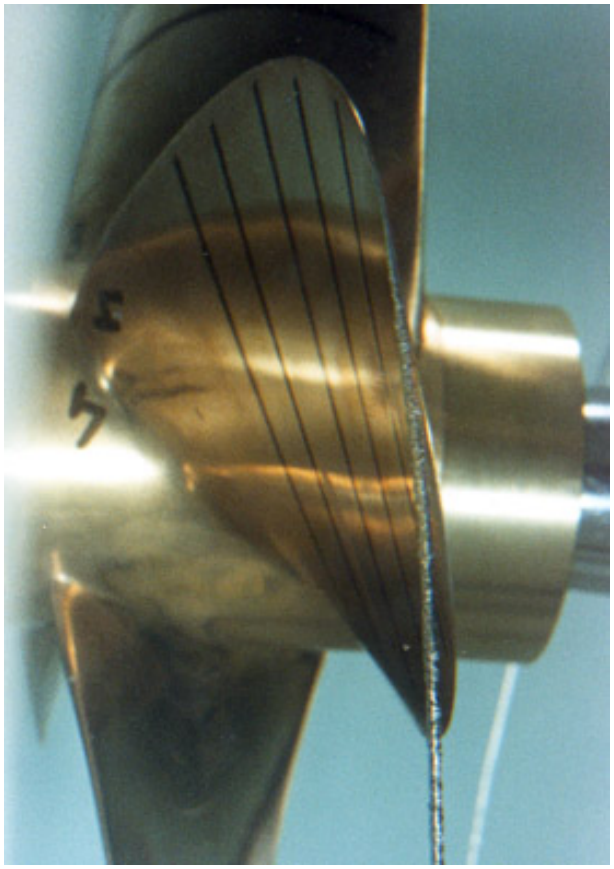

Figure 9.17: The cavitating core of a tip vortex behind a propeller

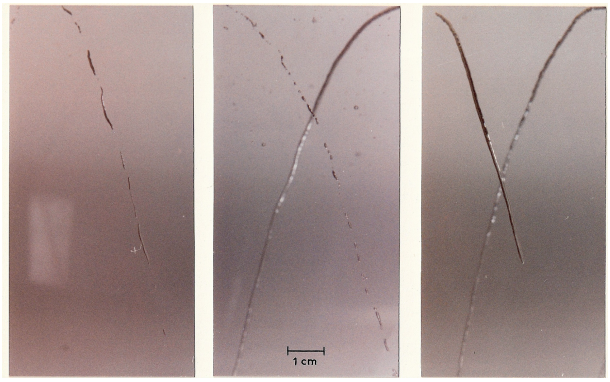

Figure 9.18: Desinent tip vortex cavitation

9.5.1 The cavitating radius as a criterion to define inception

The relation between the cavitating vortex radius and the pressure for a given vortex can be explored to define inception in an alternative way. When the relation between the pressure and the cavitating radius can be measured a diagram like Fig. 9.19 is found.

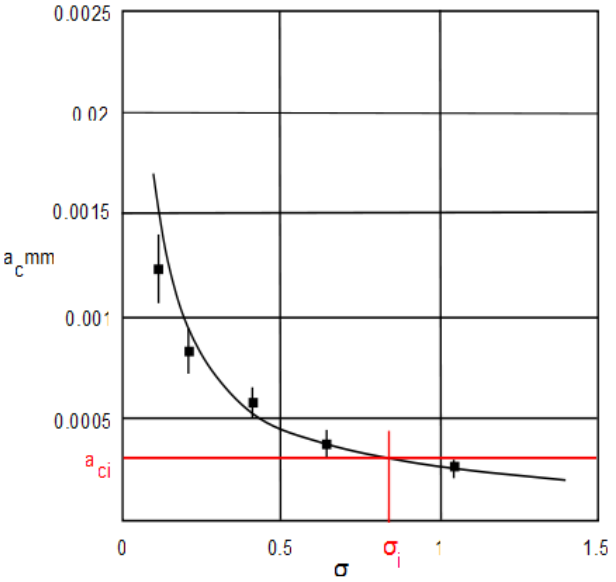

Figure 9.19: The radius of the cavitating tip vortex as a function of the pressure

When inception is now defined as the occurrence of a certain minimum radius a_{ci} the inception pressure or cavitation index σ_i can be read from the regression curve through the measured points.

When the regression curve is known, e.g. as eq.9.19, only one or a few measured points are necessary to find an inception pressure. This approach has been explored ([41],[54]), but theoretical relations were not yet very consistent with measured data.

Note that the definition of a certain minimum radius at inception for both model and full scale does not remove the differences in inception index between model scale and full scale. In eq.9.19 the cavitation index at model and full scale would be the same when both vortex radius and inception radius scale with the scale ratio. For the vortex radius this is plausible, byut not for the inception radius.

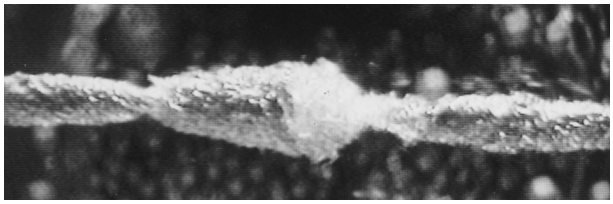

Figure 9.20: Distortions on a cavitating vortex of constant diameter

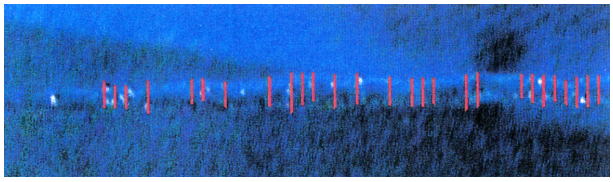

Figure 9.21: Determination of the diameter of a cavitating vortex by image recognition

There is another difficulty in this approach. The cavitation radius is often not very consistent. Even in a seemingly stable vortex local instabilities and small pressure fluctuations cause disturbances in the cavitating vortex, as illustrated in Fig. 9.20.

So in case of a propeller the radius of the tip vortex has to be determined using automatic image recognition, as shown in Fig. 9.21.

This was tried in [58],but the repeatability of the inception pressure was still not better than with visual observations. This is mainly due to the asymptotic nature of the cavitating radius close to inception. Small deviations of the inception radius lead to large variations of the inception pressure and these variations in radius occur especially when the radius is small. At lower pressures the cavitation radius increases, but near the propeller tip becomes increasingly non-cylindrical, as illustrated in Fig. 9.22

It can therefore be concluded that no standard method for inception of tip vortex cavitation is available yet. Visual observation at high air content is the current practice in cavitation tunnels, acoustic measurements are most appropriate at full scale. The repeatability and accuracy of both methods is still insufficient.

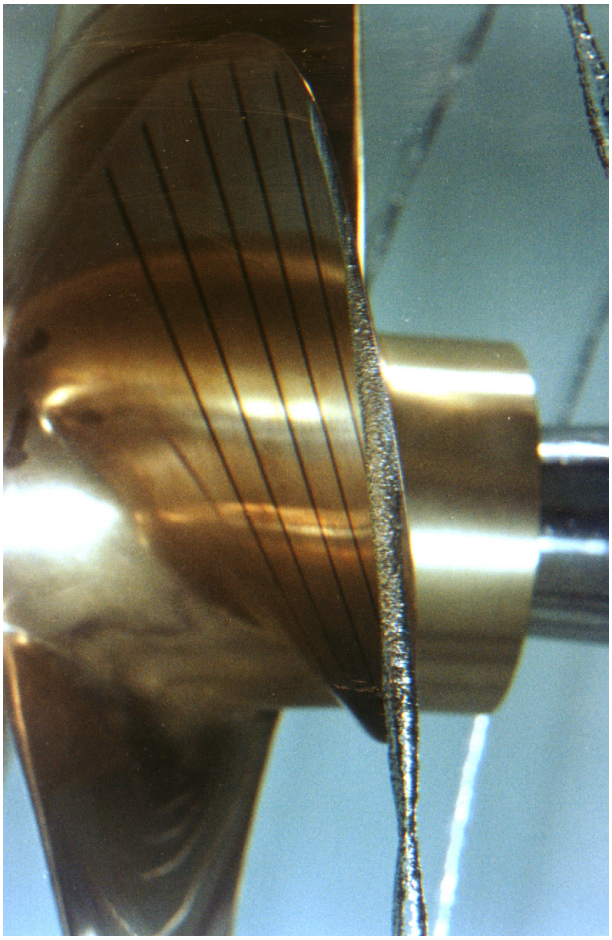

Figure 9.22: Non cylindrical tip vortex at lower pressures

9.6 Origins of a tip vortex

Until now the origin of the tip vortex has been taken as the roll-up of the trailing vorticity behind a wing or propeller blade. This is the common source of tip vortices at some distance behind the tip, although inception occurs close to the tip (Fig. 9.17).

In special cases the cavitating vortex remains detached from the tip, as shown in Fig. 9.23. However, this may also be due to a lack of nuclei, because addition of nuclei often connects the cavitation with the tip

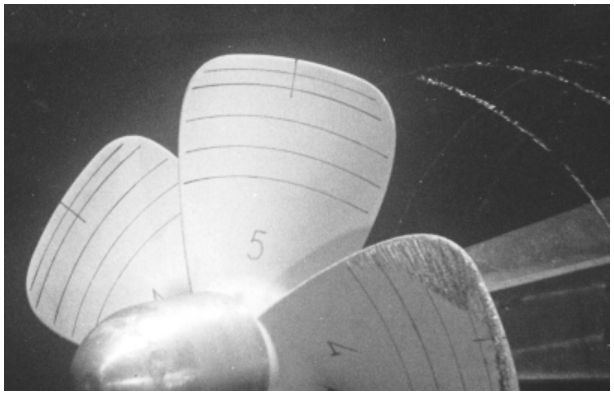

Figure 9.23: Detached tip vortex cavitation

and the origin of the vortex still is vortex roll-up at the tip. Detached cavitation can still be expected because the roll-up takes time to decrease the minimum pressure to the inception pressure. This is especially the case when the propeller tip is unloaded.

The cavitating tip vortex which consists of rolled-up vorticity from the trailing edge of the propeller blade is called a *trailing vortex cavitation.*

Another source of a tip vortex is local separation at the tip of the blade. This separation depends on the tip loading and on the tip geometry. This tip vortex will be called a *local tip vortex.* On moderately or heavily loaded tips this vortex coincides with the trailing tip vortex and thus causes attached vortex cavitation. On unloaded tips the trailing vortex and the local tip vortex may occur as separate vortices.

In cases of unloaded tips the inner radii of the propeller blade are heavily loaded. Separation of the flow at the leading edge at inner radii of a propeller blade also causes a vortex. This vortex moves towards the tip at some distance from the leading edge of the blade or foil and when cavitating this is therefore called *leading edge cavitation.* Leading edge separation occurs in streamwise direction, as sketched in Fig. 9.24.

An example of a cavitating leading edge vortex is given in Fig. 9.25.

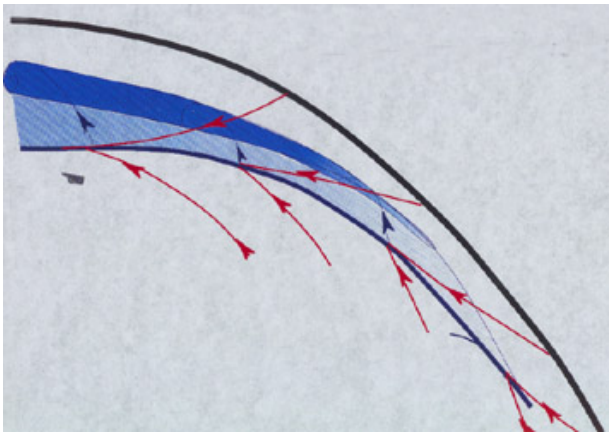

Figure 9.24: Streamlines at leading edge separation

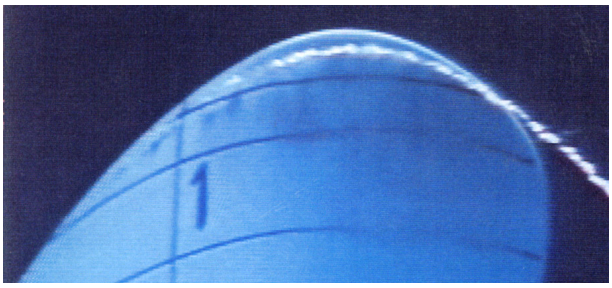

Figure 9.25: Leading edge vortex cavitation

An example of simultaneous occurrence of leading edge vortex cavitation and local tip vortex cavitation is given in video 9.26.

It is not always possible to make a sharp distinction between the different types of vortex cavitation. However, when the inception of tip vortex cavitation has to be delayed it is important to distinguish when possible, because when inception is caused by trailing vortex cavitation the tip loading has to be modified. When inception is caused by local tip vortex cavitation the shape of the tip has to be modified. And when inception is caused by leading edge cavitation the shape of the leading edge at inner radii has to be modified or the radial loading distribution has to be adjusted.

Figure 9.26: Video:Local and leading edge vortex cavitation. (stroboscopic illumination of a propeller in uniform inflow)

9.7 Effects of the nuclei content on inception of vortex cavitation

The influence of the nuclei content in the fluid on cavitation inception of vortices is strong. This is mainly because the vortex occurs in the flow, not at a surface. The presence of a surface may generate additional nuclei or disturbances in the pressure, such as in inception of sheet or bubble cavitation. But vortex cavitation depends fully on nuclei in the bulk flow and a lack of nuclei will delay the inception pressure to far below the vapor pressure. From visual observations such a delay can be recognized, because with a lack of nuclei the radius of the cavitating core at inception will be large. Similar as with bubble cavitation the few nuclei which reach the critical pressure and expand, will reach a larger size. With an abundance of nuclei the inception radius will be smaller and inception will occur less randomly. Note that for steady vortex cavitation such an abundance of nuclei can cause a collection of gas in the core. On a ship propeller inception generally takes place every revolution and this effect of gas collection is less severe.

9.8 Effects of viscosity on inception of tip vortex cavitation

As shown the minimum pressure in the center of a vortex depends on the strength of the vortex and on the radius of the viscous core. The radius of the viscous core depends strongly on the Reynolds number. There is no specific length scale or velocity related to a vortex, so the Reynolds number is generally based on the properties of the foil which generates the vortex, such as $Rn = V.c/\nu$. A crude way of estimating the dependency of the viscous core of a tip vortex is to relate it with the boundary layer thickness on the foil. Using flat plate properties of a laminar boundary layer the thickness of the boundary layer is proportional to $\frac{1}{Rn^{-0.5}}$. For a turbulent boundary layer the boundary layer thickness is proportional to $Rn^{-0.2}$.

If we take the simplest Rankine vortex model the minimum pressure in the vortex is inversely proportional to a_v^2 (equation 9.13), and the inception index σ_i is therefore proportional to $Rn^{0.4}$ in the turbulent case and to Rn in the laminar case. Measurements on foils indicated a Rn-dependency of the inception index with a power of about 0.35 ([47]). So the relation with the turbulent boundary layer thickness is not very strong.

The inception of propeller tip vortices at model scale can be compared with full scale data. This results in an empirical exponent for the Reynolds dependency of vortex inception for different facilities. The values are mostly between 0.25 and 0.4. Note that the full scale

data have an even higher uncertainty than the model data.

It has to be kept in mind that in model experiments the variation in Rn number is much smaller than required for the extrapolation. In model tests the maximum variation in Rn number is about factor 3. When the Froude number is maintained the Reynolds number scales with $\alpha^1.5$, in which α is the scale ratio. With a scale ratio of 25 this means that $Rn_{ship}/Rn_{model} = 125$! So a single exponent of the Reynolds number is a far shot indeed.

9.9 Leading edge roughness and tip vortex cavitation

When the boundary layer thickness affects the minimum pressure in a tip vortex, the state of the boundary layer will also have an affect. When the boundary layer is laminar on a wing tip, the boundary layer will be thinner and a lower minimum pressure is expected and thus earlier cavitation inception . However, due to the same laminar boundary layer there will be a lack of nuclei in the vortex core, which is delaying cavitation inception. The latter results in detached cavitation at inception (Fig. 9.23), probably because the nuclei in the bulk fluid need time to move towards the vortex core.

Application of leading edge roughness in the tip region makes the boundary layer turbulent, resulting in an increase of the minimum pressure and thus a delay of inception [28]. This applies only when in both cases wit and without roughness the boundary layer is turbulent. When the boundary layer is laminar at the propeller tip, cavitation inception may be strongly delayed by the absence of nuclei and a main effect of the roughness is the generation of nuclei in the tip vortex region, which also often results in attached tip vortex cavitation (Fig. 9.17) [40].

The precise structure of a cavitating tip vortex at inception is still unclear, and the inception conditions remain a topic for research. Experiments are very difficult because it is not possible to directly measure the pressure in the tip region due to its sensitivity for disturbances, while the region of minimum pressure is very small. It is expected that CFD can give more insight in the parameters controlling tip vortex inception.

9.10 Calculations of inception of tip vortices using CFD

The rapidly increasing application of CFD has also been applied to the tip vortex of a non-cavitating propeller. The advantage of CFD is that the minimum pressure can be calculated in the vortex center and thus that it can be correlated with inception measurements. The validation of the CFD calculations has to be done by correlating the velocities around the core region.

Tip vortices are calculated in the non-cavitating state. Application of CFD to cavitating tip vortices is still not done. An example of such a calculation on a rectangular foil tip is given in Fig. 9.27.

A typical graph of the velocities in a cross section of the vortex is given in Fig. 9.28.

In the validation with experiments the focus was on the maximum or peak velocity around the vortex and a good correlation was found, provided a proper grid resolution and turbulence model was used. The grid resolution is very important for the calculation of the vortex flow, because the region of low pressure is very small. This is illustrated in Fig. 9.29. It

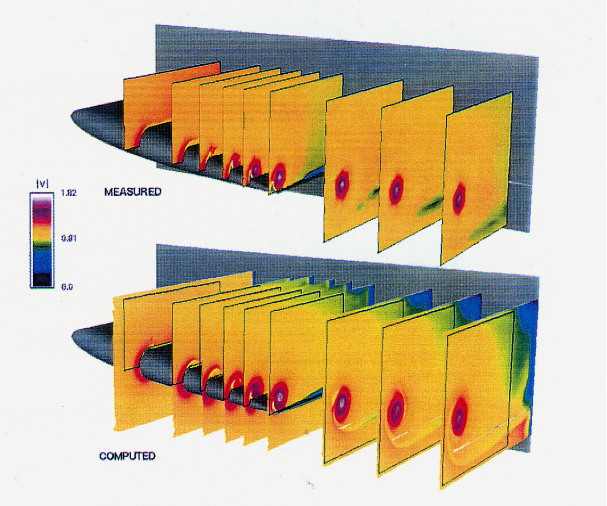

Figure 9.27: Calculated Vortex Flow on the tip of a rectangular foil [11]

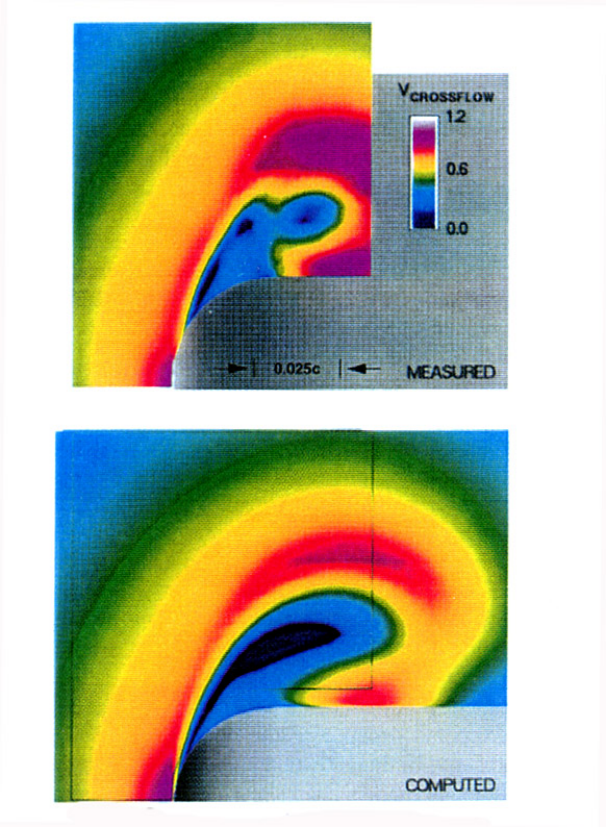

Figure 9.28: Velocity distributions in a plane perpendicular to the vortex. [11]

is obvious that the low pressure region has to contain sufficient elements to predict the pressure there correctly.

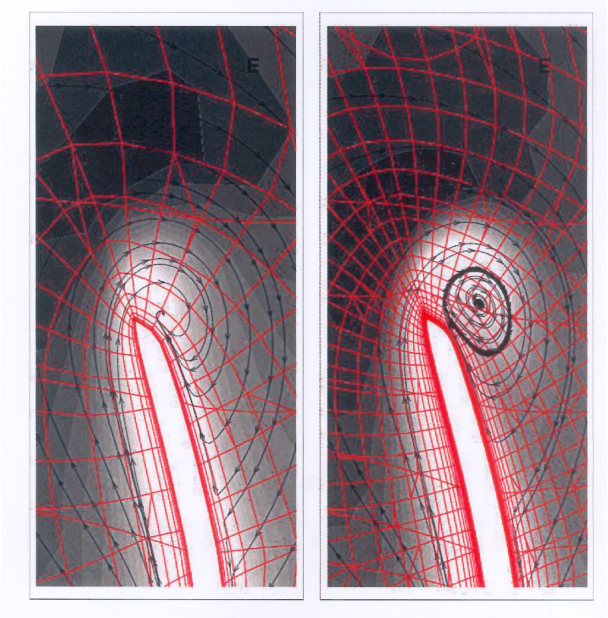

Figure 9.29: Grid refinement in the vortex region (courtesy of National Aerospace Lab. NLR in the Netherlands)

This requires such a fine grid density that local grid refinement is necessary for sufficient resolution. This requires knowledge of the position of the vortex core, so the grid refinement is therefore applied in steps, following the position of the vortex.

The final validation of such calculations is the prediction of the minimum pressure, which would mean the prediction of cavitation inception. Until now, however, the correlation of the experimental inception pressure with the calculated minimum pressure in a tip vortex is still bad, even in steady conditions and on simple forms like foils. This may be due to the calculations ([60]), but also due to the nuclei content in the experiments. This requires further investigations before reliable predictions of tip vortex inception can be made. In unsteady conditions, such as occur on a propeller in a wake, calculations of the inception pressure of the tip vortex are still to be developed.

Figure 9.30: Cavitating tip vortex near the rudder in a cavitation tunnel (courtesy VWS Berlin)

9.11 Implosion of vortex cavitation

Tip vortices are considered harmless for erosion, although they often hit the rudder (Fig.9.30).

The cavitating tip vortex folds itself around the leading edge of the rudder. The part along the rudder collapses in a distributed way and is generally not erosive. The cavitating tip vortex continues perpendicular to the rudder surface and the two parts on each side of the rudder reconnect downstream of the rudder. The reconnection is often with a knuckle, because circulation around the rudder moves the flow upwards on one side and downward on the other side of the rudder.

Still vortices may implode on the rudder. When a cavitating vortex core implodes the vortex becomes unstable and the cavitating vortex core breaks up into elements of a certain length. When these elements are small, the erosive energy is limited. When these elements are large the implosion can be erosive.This seems especially the case on vortices generated on the rudder itself, such as vortices from corners and from corners at a rudder horn. Cavitating hub vortices

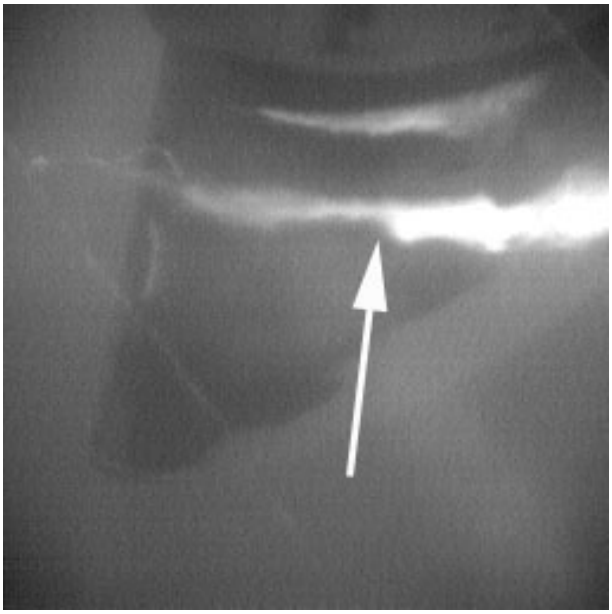

Figure 9.31: Cavitating hub vortex on a rudder at full scale (rudder to SB)

may also collapse on the rudder, especially when the rudder is at an angle. An example of a cavitating hub vortex at full scale is given in Fig. 9.31. In that picture the cavitating hub vortex is stenghtened by a low pressure region on the propeller and a collapse near the trailing edge of the propeller.

Erosivity of a cavitating vortex is even explored in erosion studies using a vortex cavitation implosion. The vortex is generated perpendicular to the eroded surface and implosion is then studied by rapidly increasing the pressure. ([4]). In that case long elements of the cavitating core collapse on the surface and cause erosion.

Tip vortex implosion also generates noise. This can be a problem in case of excessive tip vortex cavitation, where the cavitating tip vortices collapse in the vicinity of the hull. A special type of noise generation was found by Maimes. In his case it seems that waves on the surface of the cavitating vortex cause noise with discrete frequencies [46]. For lower

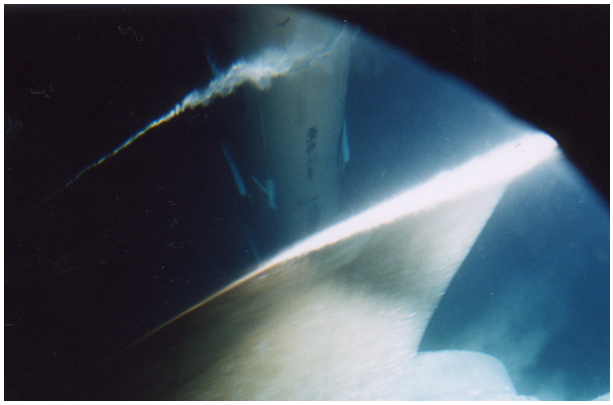

Figure 9.32: Cavitating tip vortex in the top region of a propeller in a wake

frequencies such a mechanism has been held responsible for tip vortex induced pressure fluctuations [63]. In certain circumstances tip vortex cavitation can cause "broadband noise", which is an increase in noise level in frequencies between about the third and fifth blade harmonic. The cause is still unknown, but Bosschers is also looking at wave oscillations on the cavitating vortex surface [9]

In case of a propeller behind a ship the tip vortex increases and decreases in strength during a revolution. This causes dynamic behavior of the cavitating tip vortex, often including implosion. An example is given in Fig.9.32)

This behavior is sometimes related to vortex bursting, but it is not. In case of vortex bursting the vorticity disappears due to viscous dissipation. In this case the vortex cavitation and thus also the vortex continues downstream. Only the strength of the vortex varies with the blade position. An illustration of the dynamics of such a varying vortex strength on the cavity dynamics is given on the high speed observation on a containership.

Figure 9.33: Video:Vortex cavity dynamics when a propeller blade passes a wake peak